ELSEVIER

Journal of Alloys and Compounds 394 (2005) 13–18

Journal of ALLOYS AND COMPOUNDS

www.elsevier.com/locate/jallcom

Analysis of the effects of thermal treatments on $CaHPO_4$ by ^{31}P NMR spectroscopy

B. Louati, F. Hlel, K. Guidara*, M. Gargouri

Laboratoire de l'état Solide, Faculté des Sciences de Sfax, BP 802, 3018 Sfax, Tunisia

Received 16 September 2004; received in revised form 19 October 2004; accepted 19 October 2004
Available online 8 December 2004

Abstract

The compound $CaHPO_4$ was obtained by slow evaporation at room temperature. The sample was characterised by X-ray diffraction, differential scanning calorimetry and ^{31}P MAS NMR spectroscopy at different annealing temperature. At room temperature, the observed values of the ^{31}P NMR chemical shift for the title compound are found to be −1.6, −0.4 and 1.4 ppm with the proportions 1/4, 1/2 and 1/4, respectively, revealing the presence of three non-equivalent phosphorus sites in the structure. The ^{31}P NMR investigation at different annealing temperatures points to a conversion of $(HPO_4{}^{2-})$ into $(P_2O_7{}^{4-})$ at high temperature.

Keywords: $CaHPO_4$; Diphosphate; Thermal treatments; ^{31}P NMR spectroscopy

1. Introduction

$CaHPO_4$ is of considerable biological importance in bones and teeth, and finds practical uses in dental cements and restorative materials [1]. More recently, it has been investigated as protonic conductors [2,3]. The structures consist of $CaHPO_4$ chains bonded together by $Ca\cdots O$ bonds and three types of hydrogen bonds [4,5]. Ca(1) is coordinated to seven oxygen atoms in an approximately pentagonal bipyramid but Ca(2) is coordinated to eight oxygen atoms. This sample exhibits an irreversible chemical process at high temperature consisting in the formation of diphosphate $Ca_2P_2O_7$. The complex monophosphate $(PO_4)^{3-}$ and diphosphate $(P_2O_7)^{4-}$ ions have been used as building blocks for a wide variety of crystal phases with a wide spectrum of physical and chemical properties. Both crystalline and glass monophosphate- and diphosphate-based materials have gained much interest as promising nonlinear optic materials, high-temperature ionic conductors, solid electrolytes for high energy density batteries, ion exchange materials and catalysts.

In this work, the $CaHPO_4$ compound has been prepared and characterised by XRD (X-ray diffraction) and NMR (nuclear magnetic resonance) spectroscopic techniques. On the one hand, at room temperature, the structural environments of the P atoms have been analysed using NMR spectroscopy. On the other hand, in order to investigate and discuss the irreversible chemical process at high temperature consisting in the formation of diphosphate $Ca_2P_2O_7$, we have undertaken a ^{31}P NMR study of a series of compounds with different thermal treatments.

2. Experimental

2.1. Synthesis reaction

Alkaline earth hydrogen phosphate $CaHPO_4$ was obtained by spontaneous reaction at room temperature of a stoichiometric mixture of $Ca(NO_3)_2$ and $NH_4H_2PO_4$ in water conform to the following scheme:

$$Ca(NO_3)_2 + NH_4H_2PO_4 \rightarrow CaHPO_4 + 2NO_3{}^- + NH_4{}^+ + H^+$$

Slow evaporation of the solution leads to the formation and precipitation of the compound. The powder was warmed at 353 K for few hours to eliminate the humidity. The sample

---

* Corresponding author.
E-mail address: kamelguidara@yahoo.fr (K. Guidara).

0925-8388/$ – see front matter © 2004 Elsevier B.V. All rights reserved.
doi:10.1016/j.jallcom.2004.10.025

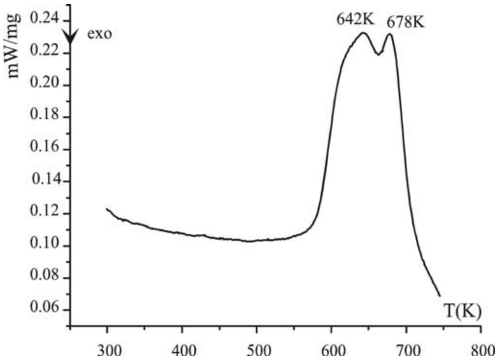

Fig. 1. Differential scanning calorimetry of $CaHPO_4$ between 300 and 750 K.

was characterised by X-ray powder patterns, differential scanning calorimetry and ^{31}P NMR spectroscopy.

3. Results and discussion

3.1. Crystalline parameters

X-ray powder diffractogram reveals that the synthesised compound is the anhydrous form of $CaHPO_4$. It crystallises in the triclinic system ($P\bar{1}$ space group) with unit cell parameters: $a = 6.91(1)$ Å, $b = 6.63(3)$ Å, $c = 6.99(3)$ Å, $\alpha = 96.32^\circ$, $\beta = 103.87^\circ$ and $\gamma = 88.37^\circ$, $V = 309.29$ Å^3 which are in good agreement with the literature values [2–4].

3.2. Calorimetric study

The calorimetric study of $CaHPO_4$ has been realised between 300 and 750 K using a NETZSCH 204 differential scanning calorimeter. Fig. 1 represents the diagram obtained at increasing temperature for a fresh preparation. One endothermic region due to phase transformation in the solid state of the sample was recorded. This region is in the 550–750 K range with a large change of enthalpy, $\Delta H = 24$ kJ/mol. The temperature anomaly is a combination of two consecutive broad peaks at 642 and 678 K. The DSC heating results are in agreement with the literature [6].

3.3. ^{31}P NMR investigation

In order to study the temperature dependence of the progress of the thermal decomposition, we have prepared a set of samples with different thermal treatments. The species are heated in air at atmospheric pressure for 24 h at fixed temperatures ranging between 273 and 723 K. The ^{31}P NMR experiments are performed on a Bruker MSL 300 ($B = 7.1$ T) spectrometer working at 121.49 MHz. The powdered samples are pocketed in the rotors and subjected to a spinning speed of 8000 Hz. A ZG sequence program (zero go) are used with a $\pi/2$ pulse length of 3 μs. NMR acquisition conditions are reported in Table 1. The ^{31}P CP MAS spectra were obtained by means of the standard cross-polarisation pulse technique followed by ^1H high-power decoupling. For the recorded spectrum, a contact time of 1 ms and a period between successive accumulations of 2 s were chosen. The number of scans was 32832 (Table 1).

Table 1
Experimental conditions

	ZG (MAS)	CP MAS
Pulse length (μs)	15.6	15.6
Dead time (μs)	10	10
Recycle time (s)	5	2
Resonance frequency (MHz)	121.49	121.49
MAS spinning speed (Hz)	8000	8000
Number of scan	720	32832
Number of digitised points	4096	4096
Referencing 0 Hz	H_3PO_4 (85%)	H_3PO_4 (85%)

The structure of the sample consists of $CaHPO_4$ chains bonded together by Ca–O bonds and three types of hydrogen bonds. Two distinct sets of pairs of PO_4 units are found in each primitive cell (Fig. 2). In the $P(1)O_4$ group the O(2)–P(1)–O(4) angle is less than the tetrahedral angle. Two other O–P(1)–O angles less than the tetrahedral angle involve oxygen O(1). In the $P(2)O_4$ group, P(2)–O(6) and P(2)–O(7) are the longest P–O distances and are about equal with an average value of 1.547 Å. The only O–P–O angle less than 109.5° in the P(2)–O_4 group involves O(6) and O(7). Concerning the three types of hydrogen bonds, one type of hydrogen bond, O(1)–H(2)···O(5), is normal but is at the short end of the normal range with O(1)···O(5) = 2.565(1) Å, one, O(7)···H(1)···O(7′), is very short with O(7)···O(7′) = 2.458(2) Å, H(1) is placed in the centre of symmetry in this hydrogen bonds with O(7)···H(1) = O(7′)–H(1) = 1.23 Å and O(7)–H(1)–O(7′) = 180° [7] and one, O(6)–H(3)···O(8) where O(6)···O(8) = 2.669(1) Å, is the normal range but is presumed to be statistically disordered with hydrogen covalently bonded to half of the O(6) atoms on the average [4,5].

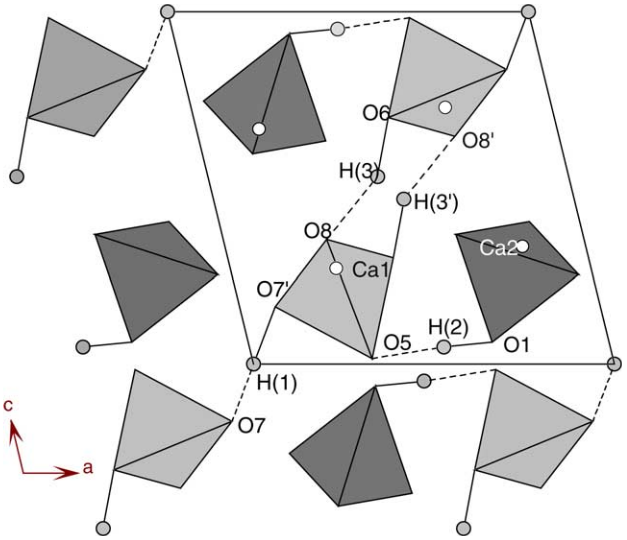

Fig. 2. [0 1 0] view of the $P\bar{1}$ structure of $CaHPO_4$, emphasising the hydrogen-bonding schema and the PO_4 tetrahedra pattern.

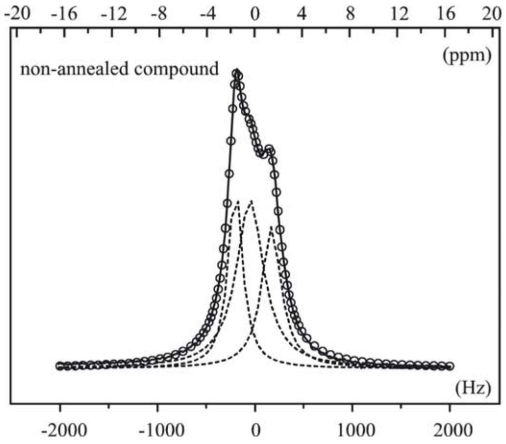

Fig. 3. Deconvolution of the ^{31}P NMR spectrum for the non-annealed compound.

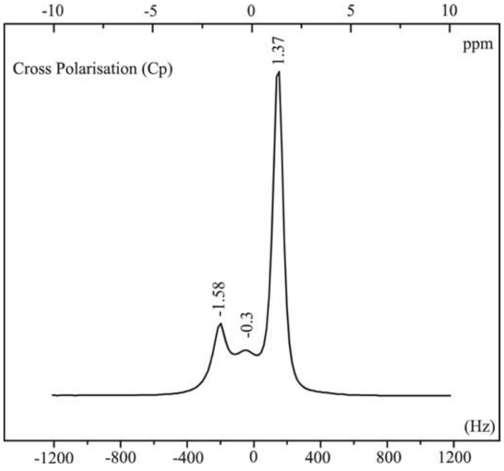

Fig. 4. ^{31}P CP MAS NMR patterns of the non-annealed compound.

Fig. 3 represents the ^{31}P NMR spectrum of the starting sample. The spectrum can be simulated by mixing three Lorentzian functions at the positions −1.6, −0.4 and 1.4 ppm in the proportions 1/4, 1/2 and 1/4, respectively. Simulation data results are listed in Table 2, scatters and continuous line correspond to the calculated and the experimental data, respectively; the dotted lines represent the Lorentzian peaks. It should be noted that the chemical shift of ^{31}P MAS NMR peaks corresponding to the non-annealed compound are in agreement with the observations by several authors on different apatites [8–10] and with the known hydroxyapatites (e.g. $Sr_{10}(PO_4)_6(OH)_2$, $Pb_{10}(PO_4)_6(OH)_2$, etc.) which δ_{iso} is in the range of 0.72; 2.9 ppm. The pure phase, ($Cd_{10}(PO_4)_6(OH)_2$), is most deshielded of the hydroxyapatites and presents a unique isotropic signal at $\delta = 12.2$ ppm [11–13].

The ^{31}P NMR spectrum of $CaHPO_4$ reveals the presence of three distinct environments of ($PO_4{}^{3-}$) in the sample. In order to enhance the multinuclear signal intensities, cross-polarisation (CP), involving the transfer of magnetisation from abundant nuclei, usually from protons, to the dilute nuclei (e.g. ^{31}P, ^{13}C, ^{29}Si), which also reduces the recycle delays, can be used. The Hartmann–Hahn (HH) matching condition for CP, $\omega(^1H) = \gamma(^1H)B_1(^1H) = \gamma(^{31}P)B_1(^{31}P) = \omega(^{31}P)$, was optimised for ^{31}P NMR (Fig. 4). The CP NMR pattern is obviously characterised by the presence of three peaks placed at −1.58, −0.3 and 1.37 ppm (Table 2). This result matches well with the previously reported results and confirm the presence of three phosphorus sites observed in the spectrum recorded using (ZG) sequence program.

The ^{31}P NMR spectroscopy results seem to be in a disagreement with the structural evidences. In fact, NMR investigation reveal the presence of three phosphorus sites but only two distinct sets of pairs of PO_4 units are found in the primitive cell by X-ray investigation.

A careful study of the crystallographic data shows that H(3) is presumed to be statistically disordered with hydrogen covalently bonded to half of the O(6) atoms on the average. Two configurations should, respectively, show H(3) bonded to O(6) only and to O(6′) only. The two tetrahedra of P(2) and P(2′) are inequivalent so when H(3) links to one of them, two different groups $HPO_4{}^{2-}$ and $H_2PO_4{}^{-}$ are formed in the structure. In the NMR time scale, the $HPO_4{}^{2-}$ and $H_2PO_4{}^{-}$ entities are inequivalent and conduce to the appearance of two distinct peaks in the spectrum, nevertheless the X-ray diffraction picture is an average one, H(3) and H(3′) seem to be simultaneously occupied in the X-ray time scale leading to a single phosphorus type. In conclusion, in the NMR time scale three distinct phosphorus types are present in the unit crystallographic cell whereas two phosphorus types are detectable by X-ray technique. It results that the B peak can be unambiguously attributed to the $P(1)O_4$ set of pairs and the A and C peaks correspond to the P(2) and P(2′) tetrahedra.

At high temperature, the $MHPO_4$ compounds exhibit an irreversible process consisting in the dehydration–condensation of the monohydrogen phosphate leading to the formation of the diphosphate $P_2O_7{}^{4-}$. This irreversible process occurs at $T = 723$ K in the case of $CaHPO_4$ [1,14].

Table 2
Deconvolution parameters of the ^{31}P NMR spectrum for the starting compound

Peak	Position (±0.5 ppm) (ZG MAS)	Position (±0.5 ppm) (CP MAS)	Normalised area (%) (ZG MAS)	Linewidth (±10 Hz) (ZG MAS)
A	−1.6	−1.6	26	176
B	−0.4	−0.3	47	342
C	1.4	1.4	27	240

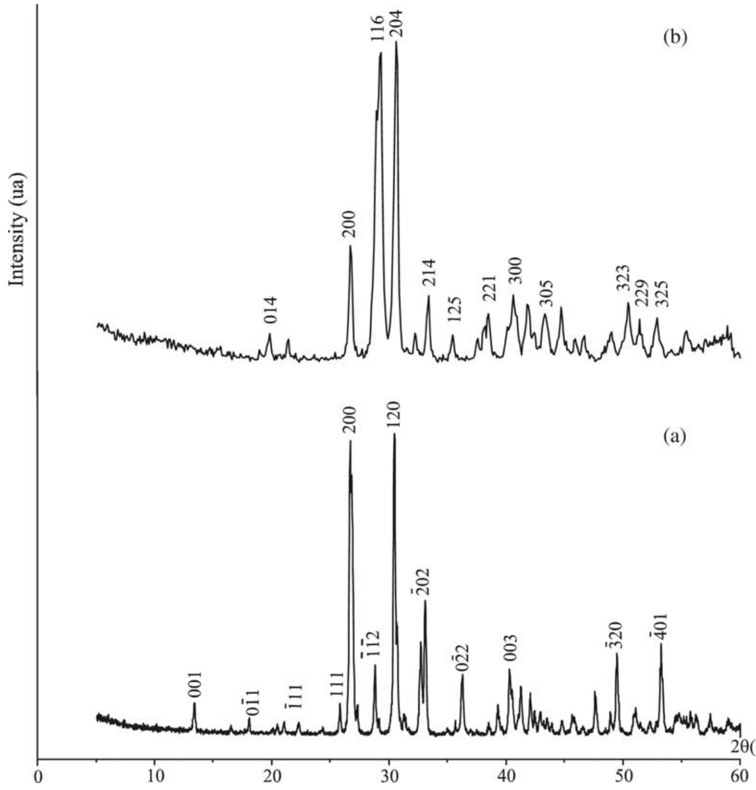

Fig. 5. X-ray powder diffraction pattern of: (a) non-annealing compound $CaHPO_4$ and (b) $CaHPO_4$ annealed at $T = 723$ K for 24 h.

Table 3
Deconvolution parameters of the ^{31}P NMR spectrum at different annealing temperatures for $CaHPO_4$

T (K)	Line shape	Position (±10 Hz)	Position (±0.5 ppm)	Linewidth (±10 Hz)	Normalised area (%)
300	Lorentz	−200	−1.6	176	26
	Lorentz	−50	−0.4	342	47
	Lorentz	170	1.4	240	27
373	Lorentz	−181	−1.5	182	43
	Lorentz	−26	−0.2	247	30
	Lorentz	136	1.1	362	27
473	Lorentz	−1043	−8.6	661	23
	Lorentz	−191	−1.6	150	70
	Lorentz	−37	−0.3	424	7
573	Lorentz	−1317	−10.9	87	11
	Lorentz	−1081	−8.9	118	13
	Lorentz	−189	−1.5	111	10
	Lorentz	−68	−0.5	458	66
623	Lorentz	−1330	−10.9	96	43
	Lorentz	−1100	−9	114	41
	Lorentz	−189	−1.5	62	1
	Lorentz	−136	−1.1	479	15
673	Lorentz	−1325	−10.9	91	43
	Lorentz	−1095	−9	112	43
	Lorentz	−418	−3.4	1537	14
723	Lorentz	−1325	−10.9	83	51
	Lorentz	−1096	−9	98	48
	Lorentz	86	0.7	240	1

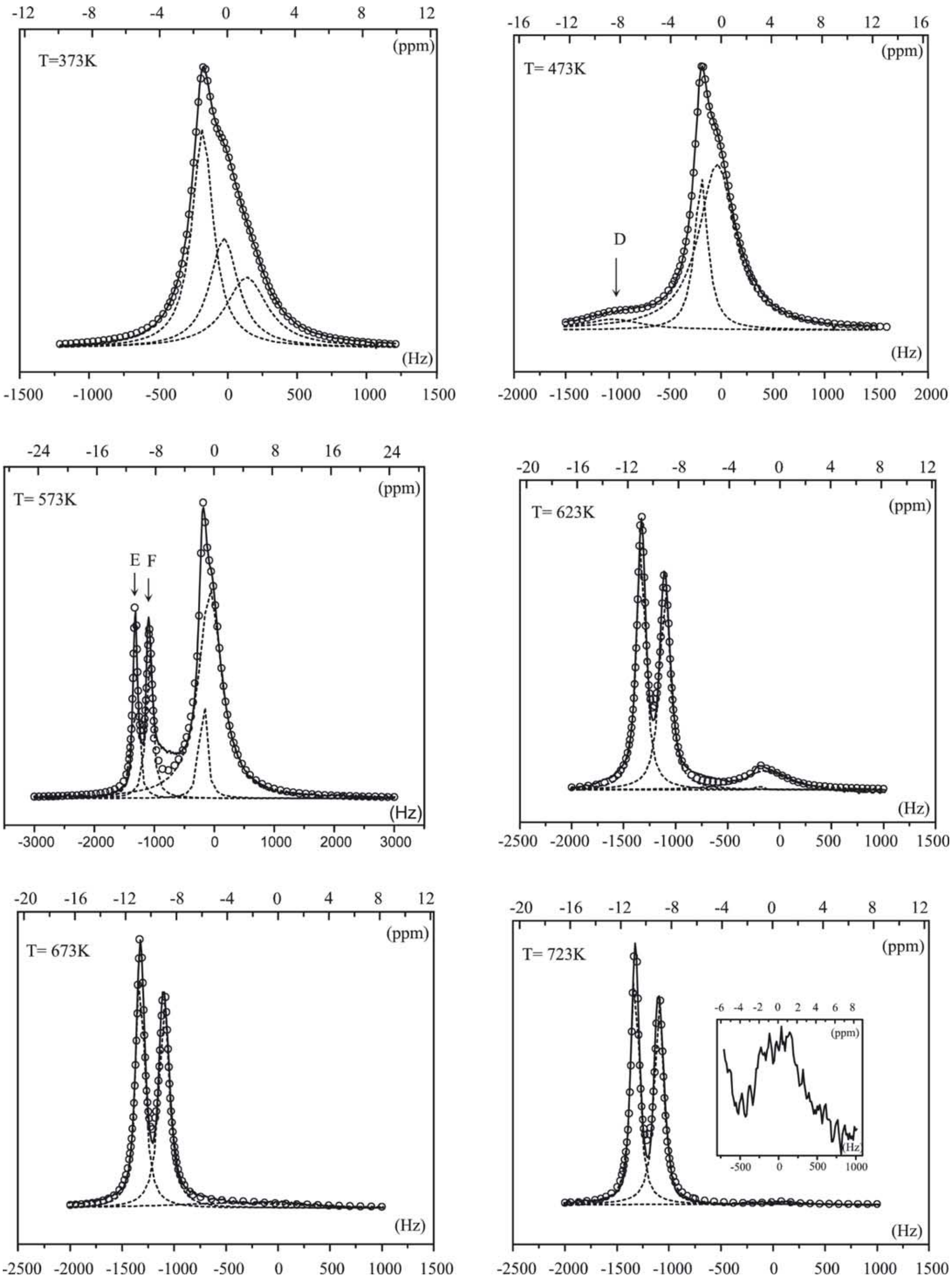

Fig. 6. Deconvolution of the ^{31}P NMR spectrum at various annealing temperatures. Inset: a zoom showing Q_0 line.

In order to study the condensation of the phosphate in the $CaHPO_4$ compound, we have prepared a set of samples with different thermal treatments. The species are heated in air at atmospheric pressure for 24 h at fixed temperatures ranging between 273 and 723 K. Fig. 5b shows the X-ray powder pattern of the annealed compound at 723 K. All the peaks can be indexed in the tetragonal system with the unit cell parameters ($a = 6.68$ Å and $c = 24.20$ Å, $P4_1$ space group). These results show a single phase and confirm the formation of the β-calcium diphosphate (β-$Ca_2P_2O_7$) phase. The cell parameters agree with the bibliographic data [15].

The set of the samples with different thermal treatment is analysed by ^{31}P NMR spectroscopy. Fig. 6 shows some NMR spectra, clearly notable changes were recorded:

i. For $T = 473$ K, the B and C lines have merged into a single line revealing the presence of drastically changes in the P tetrahedra. This change is accompanied by the ap-

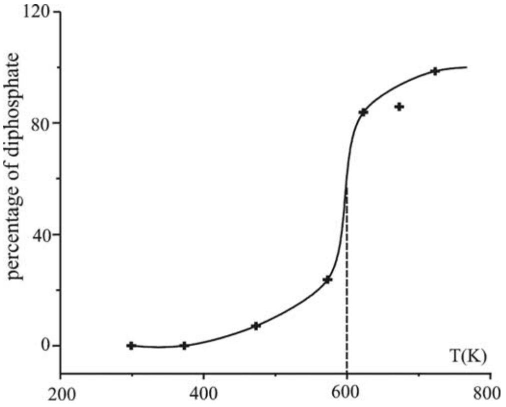

Fig. 7. Rate conversion of phosphate–diphosphate as a function of annealing temperature.

pearance of a broad line denoted D at −8.6 ppm. The large spectra modifications reflect that at high temperature the $CaHPO_4$ compound exhibits an irreversible chemical process accompanied by a dramatic change in the phosphorus environments due to the formation of the diphosphate $Ca_2P_2O_7$ conforming to the following scheme:

$$2HPO_4{}^{2-} \rightarrow H_2O + P_2O_7{}^{4-}$$

ii. With increasing temperature, the intensity of the D line increases at the cost of the A and C lines suggesting an increase of the conversion rate. At high temperatures, it splits into two components E and F of equal intensities (Table 3). The E and F lines can obviously be attributed to the phosphorus in different sites in the orthophosphate. The spectrum suggests the presence of a single orthophosphate type in the previous structure. However, the NMR results are insufficient to determine the phosphorus site that is the most sensitive to the conversion process.

iii. The ^{31}P MAS NMR spectrum recorded at 723 K shows a smaller and narrow resonance at 0.7 ppm, Q_0, and two intense resonances E and F of equal intensities at −9 and −10.9 ppm, Q_1. These resonances are assigned to the orthophosphate and pyrophosphate species, respectively. The chemical shifts seen for the last two resonances are very close to the observed value of other acid diphosphates [16,17]. In fact, the chemical shift values of the Sm diphosphates $SmHP_2O_7{\cdot}3H_2O$(II) are −11.8 and −18.3 ppm and those of La $HP_2O_7{\cdot}3H_2O$(I) are −7.6 and −16.9 ppm [18].

The percentage of diphosphate can be estimated from NMR spectroscopy. It is represented by the ratio of the area of the (E + F) peaks corresponding to the diphosphate to the total area of the spectrum, i.e. $\frac{100(E+F)}{E+F+C+A+B}$. The rate of conversion of phosphate–diphosphate as a function of temperature is plotted in Fig. 7. It increases with the annealing temperature and presents an abrupt change in the slope of the curve in the vicinity of 600 K. At $T = 723$ K, the reaction is totally achieved and reaches the maximum value (98.8%).

4. Conclusion

In this work, we have synthesised the $CaHPO_4$ compound. The sample was investigated by X-ray diffraction, DSC and ^{31}P NMR spectroscopy at different annealing temperatures.

^{31}P MAS NMR study of the non-annealed compound show three peaks A, B and C at the positions −1.6, −0.4 and 1.4 ppm in the proportions 1/4, 1/2 and 1/4, respectively, revealing the presence of three types of phosphorus in the structure. The B peak is ascribed to $P(1)O_4$ group, however, the A and C peaks correspond to the P(2) and P(2′) tetrahedra. The DSC curve of $CaHPO_4$ shows two endothermic peaks at about 642 and 678 K. According to ^{31}P NMR data evolution with annealing temperatures, the transition observed by DSC has been interpreted as an irreversible chemical process consisting in the formation of the diphosphate $Ca_2P_2O_7$.

References

[1] G.R. Sivakumar, E.K. Girija, S.N. Kalkura, C. Subramanian, Cryst. Res. Technol. 33 (1998) 197.
[2] L. Tortet, J.R. Gavarri, G. Nihoul, A.J. Dianoux, J. Solid State Chem. 132 (1997) 6.
[3] L. Tortet, J.R. Gavarri, G. Nihoul, A.J. Dianoux, J. Solid State Ionics 97 (1997) 253.
[4] B. Dickens, J.S. Bowen, W.E. Brown, Acta Cryst. B 28 (1971) 797.
[5] A. Boudjada, R. Masse, J.C. Guttel, Acta Cryst. B 34 (1978) 2692.
[6] R.A. Vargas, M. Mosquera, Revista Mexicana de Fisica 3 (1993) 450.
[7] M. Catti, G. Ferraris, Acta Cryst. B 33 (1977) 1223.
[8] J.L. Miquel, L. Facchini, A.P. Legrand, X. Marchandise, P. Lecouffe, M. Chavanaz, M. Donozzan, C. Rey, J. Lemaître, Clin. Mater. 5 (1990) 111.
[9] J.P. Yenisowski, H. Eckert, J. Am. Chem. Soc. 109 (1987) 6274.
[10] A. Rodrigues, A. Lebugle, Colloid. Surf. A: Physicochem. Eng. Aspects 145 (1998) 191.
[11] J.P. Yesinowski, J. Am. Chem. Soc. 103 (1981) 6266.
[12] B. Badraoui, M. Debbabi, R. Thouvenot, C.R. Hebd, Acad. Sci. Ser. IIC 3 (2000) 107.
[13] B. Badraoui, A. Bigi, M. Debbabi, M. Gazzano, N. Roveri, R. Thouvenot, Eur. J. Inorg. Chem. 5 (2001) 1261.
[14] A. Durif, Crystal Chemistry of Condensed Phosphates, Plenum Press, New York, 1995, pp. 23–57.
[15] N.C. Webb, Acta Crystallogr. 21 (1966) 942.
[16] N.J. Clayden, S. Esposito, P. Pernice, A. Aronne, J. Mater. Chem. 11 (2001) 936.
[17] P. Hartmann, J. Vogel, B. Schnabel, J. Non-Cryst. Solids 176 (1994) 157.
[18] S.B. Moussa, S. Ventemillas, A. Cabeza, E.G. Puebla, J. Sanz, Solid State Chem. 177 (2004) 2129.